Journal of Sustainability Science and Management
Volume 17 Number 5, May 2022: 139-148
eISSN: 2672-7226
© Penerbit UMT

PLASTICIZED CMC-AMMONIUM ACETATE BASED SOLID BIOPOLYMER ELECTROLYTE: IONIC CONDUCTIVITY AND TRANSPORT STUDY

MOHD IBNU HAIKAL AHMAD SOHAIMY[1], NURUL IZZATI ZAINUDDIN[1] AND MOHD IKMAR NIZAM MOHAMAD ISA[1,2]*

[1]Advanced Materials Team, Ionic & Kinetic Materials Research (IKMaR) Laboratory, Faculty of Science and Technology, Universiti Sains Islam Malaysia, 71800 Nilai, Negeri Sembilan, Malaysia. [2]Advanced Nano Materials (AnoMa), Ionic State Analysis (ISA) Laboratory, Universiti Malaysia Terengganu, 21030 Kuala Nerus, Terengganu, Malaysia.

**Corresponding author: ikmar_isa@usim.edu.my*
Submitted final draft: 3 November 2021 *Accepted: 31 December 2021* http://doi.org/10.46754/jssm.2022.05.011

Abstract: In this work, a plasticised carboxymethyl cellulose (CMC) solid biopolymer electrolytes (PSBEs) system was prepared via solution casting technique with ammonium acetate (NH_4CH_3COO), ethylene glycol (EG) as doping salt and plasticiser respectively. Upon addition of 35 wt.% of EG (PSBE 4), the ionic conductivity obtained is 1.81×10^{-5} Scm^{-1} which represents the optimum value for the system. The PSBE also tested at elevated temperatures and fitted to an Arrhenius equation. Fourier Transform Infrared Spectroscopy (FTIR) analysis found no significant changes to the molecular structure of CMC with addition of EG. Jonscher's power law indicates that quantum tunnelling is the well-matched model to describe ionic conduction for PSBE 4 and it appears that it is also highly ionic with good transference number obtain from dc polarisation analysis technique.

Keywords: Solid biopolymer electrolytes, carboxymethyl cellulose, plasticizer, ethylene glycol, Jonscher's power law.

Introduction

Polymer is defined as molecules that consist of repeating smaller molecules (monomers) linked together in 2-dimensional (2D) or 3-dimensional (3D) networks forming large or long molecular chains. This varying structure allows polymeric materials to achieve a wide range of physical, chemical and mechanical properties (Shrivastava, 2018). As a result, polymeric materials are gaining a lot of attention in the medical, agricultural, construction and electrochemical fields (Virya & Lian, 2021; Isa *et al.,* 2021; Yazdani *et al.,* 2018; Milani *et al.,* 2017).

In electrochemical applications especially, polymeric materials proved to be an exciting substance it can help to solve flaws with current battery technology when applied as solid polymer electrolytes (SPE). The characteristics of SPE, which can eliminate leakage issues is preferable in electrochemical applications. Another type of solid electrolyte namely inorganic composite electrolytes (ICE) can also eliminate this problem however it suffers from high brittleness and sluggish electrode-electrolyte contacts, while SPE does not suffer from similar problems which make it the better choice (Meng, Zhu & Lian, 2022).

To date, there has been plenty of research on SPE and the topic has been reported on ever since the discovery of conducting polymers in the 1970s. Most of SPEs were developed using synthetic polymers like Polyvinyl acetate (PVA a water-soluble synthetic polymer), Polymethyl methacrylate (PMMA), a transparent thermoplastic and Poly(ethylene Oxide (PEO), a polymer with many applications and FDA approval for clinical use (Sohaimy *et al.,* 2020).

However, the focus is starting to sift from these synthetic polymers for safety, environmental and cost reasons (Perumal *et al.,* 2019). Using natural polymers (biopolymers) is seen as the best alternative to synthetic polymers since it is biodegradable, non-toxic and renewable or sustainable (Mohiuddin *et al.,* 2018).

Chitosan (Kim & Lim, 2021), starch (Selvanathan *et al.,* 2021) and carrageenan

(Zainuddin *et al.,* 2020) are some examples of biopolymers that have been applied in polymer electrolyte systems. Though, cellulose-based biopolymers are more compelling since it is the most abundant natural polymer (Kim & Lim, 2021).

Carboxymethyl cellulose (CMC) is a derivative of a cellulose biopolymer that has been applied in various industries such as the food, cosmetics, textile and pharmaceutical industries (Kaewprachu *et al.,* 2022). Some properties that CMC has which make it suitable for industrial applications are that it is biodegradable, highly soluble and has good mechanical strength (Kaewprachu *et al.,* 2022; Zainuddin *et al.,* 2020).

In electrochemical applications, the presence of carboxyl group (COO) on the side chain of the CMC biopolymer can help in ionic conduction. The presence of free electron pairs of the oxygens can act as temporary coordination site for free ions to attach and subsequently improve the ionic conduction value as seen in some reports (Isa *et al.,* 2021; Zainuddin *et al.,* 2020; Rani *et al.,* 2014).

A good electrolyte is defined by how great the ionic conductivity is and CMC has very low ionic conductivity which limits the applications as an electrolyte. Several techniques can be adopted to enhance the ionic conductivity of SBE, but plasticisation techniques are an effective method to improve the ionic conductivity of a polymer electrolyte framework as it can soften the polymer backbone to make the polymer less structured (Tuan Naiwi *et al.,* 2018).

As a result, this technique was selected for study in this research paper. Ethylene glycol (EG) was selected as the plasticiser since it has a small molecular structure and can easily penetrate the polymer chain and aid in ionic conduction.

Ammonium acetate (NH_4CH_3OO) was also added as source of charge carrier. The prepared SBE was tested for its ionic conductivity, structure and ionic transport properties to determine its potential and viability for electrochemical applications.

Materials and Methods

Preparation of PSBE Film

The materials used in this work were procured from Across for CMC, Bendosen for NH_4CH_3COO and Sigma-Aldrich for EG. The materials were used as received without treatment. The CMC-NH_4CH_3COO plasticised SBE (PSBE) were prepared using a solution casting method and underwent drying process at room temperature (303K).

For starters, in the PSBE preparation process, 2 g of CMC powder was dissolved in distilled water (100 ml) before adding 0.5 g of NH_4CH_3COO and stirred continuously until a homogenous solution was obtained. The amount of salt used was based on the highest conducting sample in a previous report (Rani *et al.,* 2014).

Next, different concentrations of EG were added into the solution while stirring. Finally, the solution was poured into separate petri dishes and dried until thin film was formed (Figure 1).

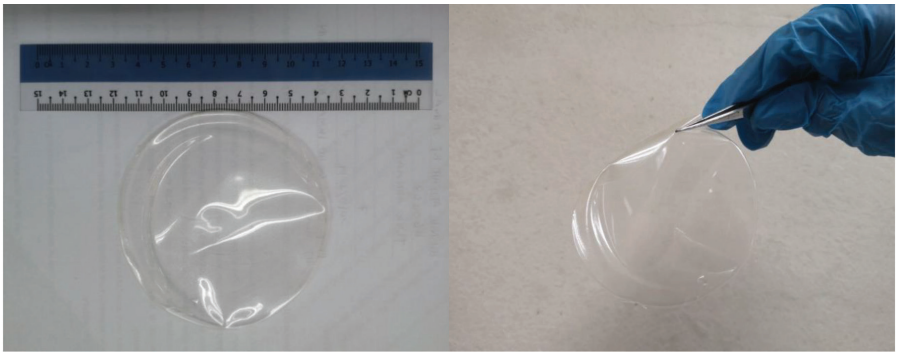

Figure 1: A highly transparent and flexible PSBE obtained via a solution casting method

To prevent sample contamination and moisture absorption, the PSBEs were then stored in a desiccator before being characterised. The designation, composition and film thickness of the PSBE is tabulated in Table 1.

Characterization of PSBE Film

Fourier Transform Infrared Spectroscopy (FTIR)

FTIR was carried out by using Varian 3100 FTIR Excalibur series attached with ATR (germanium crystal). The spectrum was recorded with wavelength ranging from 4000 cm^{-1} to 500 cm^{-1} with resolution of 4 cm^{-1}.

Electrical Impedance Spectroscopy (EIS)

The impedance measurement of CMC-NH_4CH_3COO PSBE was conducted using HIOKI IM3570-50 LCR HiTester in the frequency ranging from 50 Hz to 1 MHz and the temperature ranging from 30°C to 80°C. Spring pressured stainless steel electrodes were used in this test to hold the sample. The data obtained from this measurement was then used to determine the bulk resistance, R_b and the conductivity of the PSBE using Equation 1 (Rani *et al.,* 2014) below:

$$\sigma = \frac{t}{R_b A} \quad (1)$$

where t is the thickness of PSBE film, R_b is the bulk resistance and A is the area of the PSBE film respectively. The thickness of the PSBE films were measured using a digital micrometer gauge as tabulated in Table 1. The PSBE film was also measured at elevated temperature and fitted to Arrhenius relations (Equation 2) (citations).

$$\sigma = \sigma_0 \exp\left(\frac{-E_a}{kT}\right) \quad (2)$$

From the equation, σ_0 is the pre-exponential factor, Ea is the activation energy (eV), k is the Boltzmann constant and T is the absolute temperature (K).

Transference Number Measurement (TNM)

To further associate the effect of the plasticiser with the ionic conductivity of PSBEs, d.c. polarisation technique was used to measure the ionic transference number. This method employed dc power supply and computerised digital multimeter. The sample was place between stainless steel sample holder and connected to the power supply and computerised in series (Figure 2). During the measurement process, 1.0 V (dc) was subjected to the SBE and the resulting electric current over time was recorded through computerised multimeter.

Table 1: List of composition and designation for CMC-NH_4CH_3COO PSBE

Samples Designation	CMC (g)	NH_4CH_3COO (g)	EG (wt%)	EG (g)	Thickness, t (cm)
PSBE 0	2	0.5	0	0.0000	0.0077
PSBE 1	2	0.5	5	0.1316	0.0083
PSBE 2	2	0.5	15	0.4411	0.0088
PSBE 3	2	0.5	25	0.8330	0.0069
PSBE 4	2	0.5	35	1.3462	0.0093
PSBE 5	2	0.5	45	2.0455	0.0105

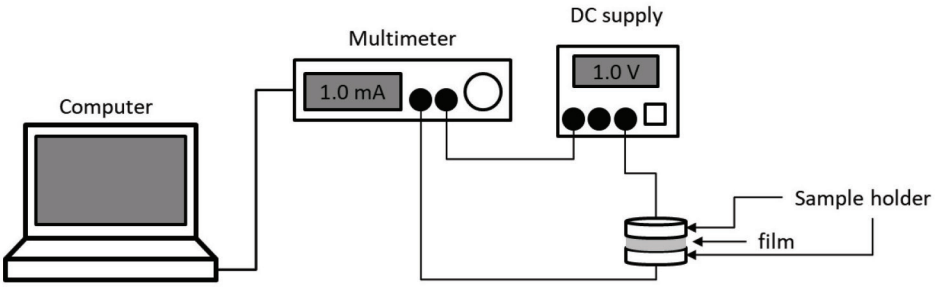

Figure 2: Dc polarization experimental setup

Results and Discussion

Ionic Conductivity Studies

The impedance data obtained from EIS testing was plotted into Cole-Cole plot for analysis and Figure 3 shows the Cole-Cole plot of PSBEs system at room temperature. All samples show similar impedance shape which could be represented with different electronic components where the semi-circle (arc) represents the combination of capacitive and resistive components of the PSBE while the slanted straight line represents the constant phase element (CPE) of the PSBE (Muchakayala *et al.,* 2017).

As seen from the figure, the PSBE 4 shows the smallest semi-circle compared with the other samples. The bulk resistance, R_b of the PSBE was determined by finding the value of real impedance from the intercept between the semi-circle and the straight line. This infers that PSBE 4 has smaller resistance compared to the rest of the PSBE films.

Figure 4 shows the ionic conductivity for PSBE films at room temperature. The ionic conductivity for PSBE 0 has the ionic conductivity of 0.12×10^{-5} Scm^{-1} and increase up to the 1.81×10^{-5} Scm^{-1} (optimum value) at PSBE 4. The increased ionic conductivity with addition of EG is believed due to enhancement of ionic mobility where the presence of plasticiser improves ionic migration of free ions by decreasing polymer-polymer chain interaction and increasing segmental motion (Ganesan *et al.,* 2018).

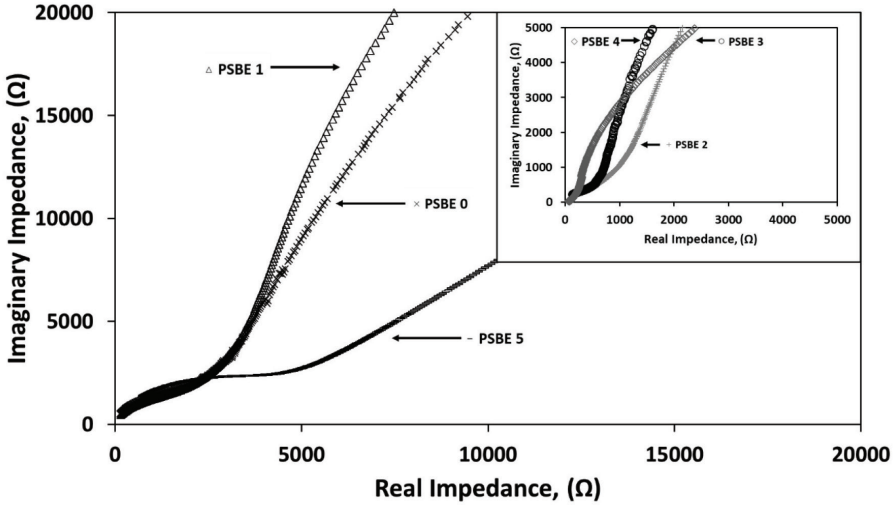

Figure 3: Impedance plot of CMC-NH_4CH_3COO PSBE

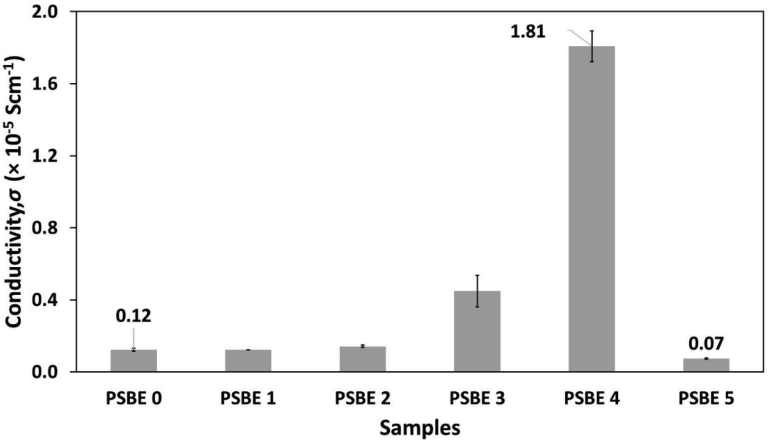

Figure 4: Variation of conductivity at room temperature for PSBE samples

On top of that, the two-hydroxyl group at the end of the plasticiser structure can also contribute to an increased coordination site. Thus, it is believed that ionic migration favours the plasticiser rich phase as seen with increased EG concentration.

However, with further increasing of plasticizer concentration (PSBE 5), the ionic conductivity decreases to 0.07 × 10^{-5} Scm^{-1}. It is believed that higher amounts of EG contribute to the overcrowding of ions (forming ion aggregates) and thus limits the mobility of ions (Sangeetha *et al.,* 2021). Similar behaviour was observed for other plasticised system reported by Hafiza and Isa (2017a) when too much plasticiser was added.

The ionic conductivity was also investigated at various temperatures ranging from 303 K to 353 K to understand in detail the possible ionic conduction mechanism. Figure 5 shows the plot of log conductivity, σ versus 1000/T for PSBE system. From Figure 5, straight lines on the graph of log conductivity, σ versus 1000/T give the regression value near to unity, $R^2 \sim 1$, which in the range of 0.95 ~ 0.99.

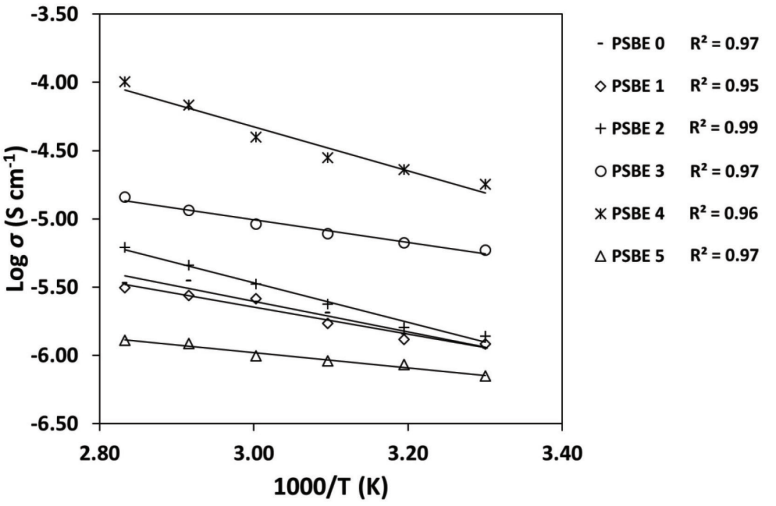

Figure 5: Conductivity variation at elevated temperature of PSBE samples

This indicates that the Arrhenius relationship between ionic conductivity and temperature was satisfied. The conductivity increased as the temperature increased is mainly due to the increase of free volumes for the motion of ions through the polymer backbone vibration.

FTIR Analysis

Figure 6 shows the Fourier Transform Infrared Spectroscopy (FTIR) spectrum of PSBEs in the region of 600 – 3600 cm^{-1}. The spectrum shows typical wavenumber peak found in CMC (Li & Yang 2019; Salama *et al.,* 2019). The broad peak at ~3350 cm^{-1} referring to O-H stretching vibration. Peak at ~2954 cm^{-1} is due to C-H stretching vibration associated with methyl and methylene group of CMCs. From the figure, the broad peak increases with increase EG concentration. This was due to the overlapping of O-H stretching vibration of EG, which was reported to be around ~3350 cm^{-1} (Guo & Zhang, 2018; Kononova *et al.,* 2018).

While the peak corresponds to the carboxylic group (COO) of CMC can be seen to peak at between 1000 and 1600 cm^{-1} where it peaked at 1585 cm^{-1} due to C=O stretching and peaked at ~1020 cm^{-1} due to C-O of the carboxyl group. Peaks of O-H stretching at ~1415 cm^{-1} and C-H stretching at ~1322 cm^{-1} was observed respectively.

Weak vibration peaked at ~900 cm^{-1} corresponds to C-H stretching. As can be seen from the figure, the C-H vibrations become apparent and shifted to lower wavenumber (882 cm^{-1}) as EG concentration increased. Second C-H peak was also observed at ~860 cm^{-1} for sample with the highest EG concentration thus forming a doublet peak which confirms the dual CH_2 group of EG (Guo & Zhang, 2018).

To further investigate the effect of EG concentrations towards the PSBE, selected FTIR spectrum peaks were given attention and the peaks at ~1585 cm^{-1} and ~1020 cm^{-1} were chosen. The two peaks mentioned correspond to COO group of CMC, which is the complexation/interaction most likely to occur in the PSBE. Both value of peaks for different EG concentration was extracted and tabulated in Table 2. From the table, both peaks show minimal or no significant changes to the wave number values with the addition of EG.

This implies that the EG did not make any interaction with the carboxyl group of CMCs, its presence just only providing a new pathway for proton (H^+ ion) transportation.

This makes the ions easily migrate through the CMC backbone and consequently enhance the ionic conductivity. However, at the highest EG concentration, both peaks appear to shift

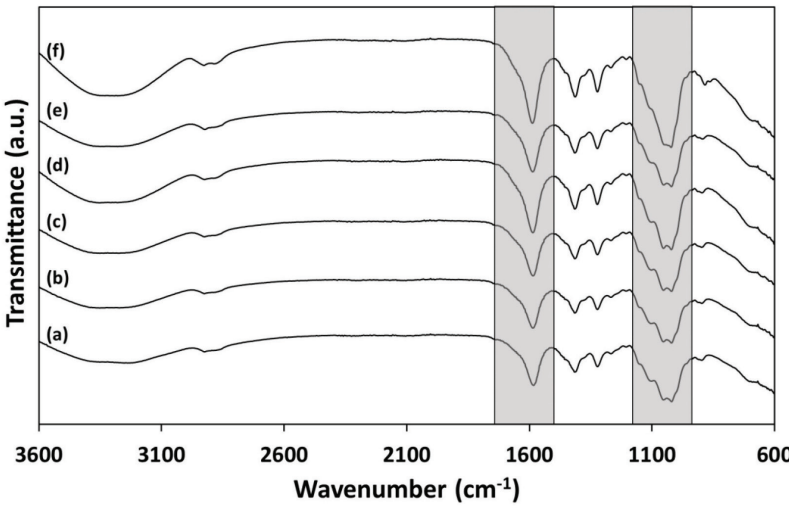

Figure 6: FTIR spectra of (a) PSBE 0, (b) PSBE 1, (c) PSBE 2, (d) PSBE 3, (e) PSBE 4 and (f) PSBE 5

Table 2: The wavenumber for C=O and C-O of the PSBE

Sample	C=O Peak (cm^{-1})	C-O Peak (cm^{-1})
PSBE 0	1583	1020
PSBE 1	1586	1021
PSBE 2	1586	1021
PSBE 3	1586	1021
PSBE 4	1587	1021
PSBE 5	1587	1022

slightly to higher wavenumber (from 1583 - 1587 cm^{-1}; from 1020 - 1022 cm^{-1}). This slight shifting is assumed to be negligible since it is within the range of FTIR resolutions. Based on this evidence, the assumption explain in previous section was justified and the ionic conduction of the PSBE is illustrated as shown in Figure 7.

Ionic Transference and Transport Model

For further evaluation on the PSBE 4 conduction behaviour, the film was tested for its conduction model and transference number. The ionic conduction modelling mechanism was analysed using Jonscher's Universal Power Law (UPL) (Equation 3).

The method of using this power law was previously explained by Hafiza and Isa (2018). Figure 8 (a) shows the relationship of dielectric loss and frequency calculated using Jonscher's UPL equation (Equations 3 and 4) at high frequency region. This frequency range was selected to minimise the effect of space charge polarisation. The exponent s in the equation ($0 \leq s \leq 1$) represents the degree of interaction between mobile ions and the lattices around them (Dhari *et al.,* 2018).

Figure 8 (b) illustrates the variation of exponent s at selected temperature where it found to be independent of temperature or near constant which was best described by quantum mechanical tunnelling (QMT) model. It is believed that the polarons (protons, H^+ and it stress field) tunnelled through the potential barrier existed between coordinating site (which in this case refers to carboxylic group of CMC) (Hafiza & Isa, 2017b).

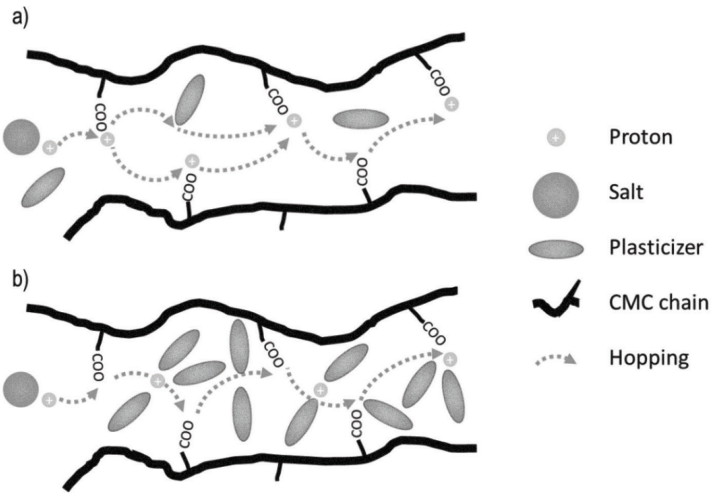

Figure 7: Schematic representing the ionic conduction in the PSBE with (a) moderate plasticiser concentrations and (b) excess plasticiser concentrations

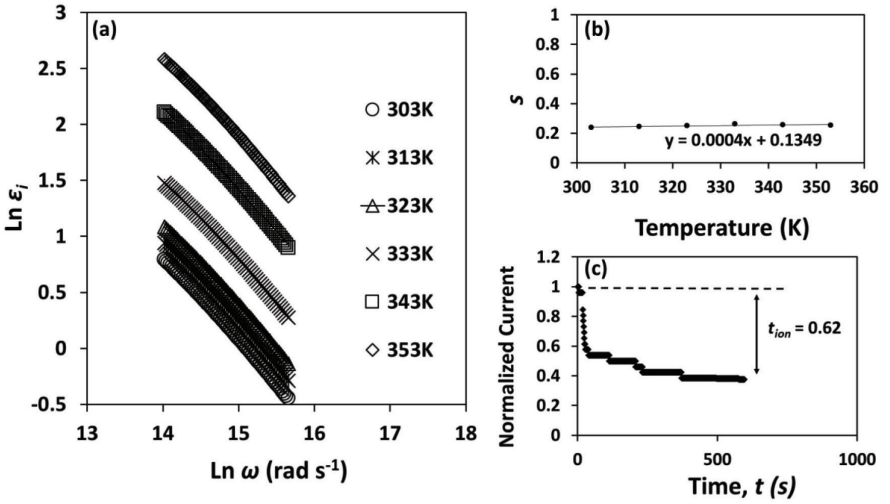

Figure 8: (a) Plot of dielectric loss vs frequency at elevated temperature, (b) plot of *s* value against temperature and (c) plot of transference number measurement

Figure 8 (c) shows the plotted dc polarisation current for PSBE 4 (the highest conducting PSBE film). As observed from the figure, the current decreases rapidly initially before plateauing after some time. This is due to the depletion of ionic species in the PSBE film and it becomes plateau when mobile species was fully depleted (Hemalatha *et al.,* 2019). The ionic transference number, t_{ion} for PSBE 4 is 0.62, indicating that the film is predominantly ionic (Hafiza & Isa, 2017c) and thus allowing more protons (H^+ ions) to take part in the conduction process.

$$\sigma_{ac} = \sigma_{dc} + A\omega^S \quad (3)$$

$$\ln \varepsilon_i = \ln \frac{A}{\varepsilon_0} + (s+1) \ln \omega \quad (4)$$

Conclusion

In this study, the PSBE system was successfully prepared using solution casting technique. The ionic conductivity increased up to 35 wt % addition of EG (PSBE 4) before it dropped at high EG addition (PSBE 5).

Based on the overall analysis, the presence of EG plastiser has only providing a new pathway for protons, H^+ transportation through the CMC branch end and the backbone to then improve the conduction process.

With higher numbers of t_{ion} as indicated from transference testing for PSBE 4 film (the highest conducting PSBE film), it is believed that high numbers of protons (H^+ ions) were supplied into the system. This enables them to form polarons and tunnel through potential barrier between complexation sites (carboxyl group) and subsequently increase the ionic conductivity.

Acknowledgements

The author would like to thank and acknowledge the staff at Faculty of Science and Technology, Universiti Sains Islam Malaysia for the service provided and to Universiti Sains Islam Malaysia (USIM) for funding this research through research grant (16619).

References

Dhahri, A., Dhahri, E., & Hli, E. K. (2018). Electrical conductivity and dielectric behaviour of nanocrystalline $La_{0.6}Gd_{0.1}Sr_{0.3}Mn_{0.75}Si_{0.25}O_3$. *RSC Advances*, *8*, 9103.

Ganesan, S., Mathew, V., Rathika, R., Muthuraaman, B., Maruthamuthu, P., Suthanthiraraj, S. A., & Kim, J. (2018).

Low-cost tetra ethylene glycol derivatives in polymer blend electrolytes for dye-sensitized solar cells with high photovoltaic conversion efficiencies. *Materials Science and Engineering: B*, *229*, 37-43.

Guo, Y. C., & Zhang, Y. H. (2018). Observation of conformational changes in ethylene glycol-water complexes by FTIR-ATR spectroscopy and computational Studies. *AIP Advances*, *8*, 055308.

Hafiza, M. N., & Isa, M. I. N. (2017a). Analyses of ionic conductivity and dielectric behavior of solid polymer electrolyte based 2-hydroxyethyl cellulose doped ammonium nitrate plasticized with ethylene carbonate. *AIP Conference Proceedings*, *1885*, 020080.

Hafiza, M. N., & Isa, M. I. N. (2017b). Studies of ionic conductivity and A.C. conduction mechanism of 2-hydroxyethyl cellulose based solid polymer electrolytes. *Journal of Sustainability Science and Management*, *2017*(Special Issue 2), 65-70.

Hafiza, M. N., & Isa, M. I. N. (2017c). Transport studies of carboxymethyl cellulose/ chitosan-ammonium bromide biopolymer blend electrolytes as an ionic conductor. *Journal of Sustainability Science and Management*, *2017*(Special Issue 2), 58-64.

Hafiza, M. N., & Isa, M. I. N. (2018). Conduction mechanism via correlated barrier hopping in EC-plasticized 2-hydro xyehyl cellulose-ammonium nitrate solid polymer electrolyte. *IOP Conference Series: Materials Science and Engineering*, *440*, 012039.

Hemalatha, R., Alagar, M., Selvasekarapandian, S., Sundaresan, B., & Moniha, V. (2019). Studies of proton conducting polymer electrolyte based on PVA, amino acid proline and NH4SCN. *Journal of Science: Advanced Materials and Devices*, *4*(1), 101-110.

Isa, M., Sohaimy, M., & Ahmad, N. (2021). Carboxymethyl cellulose plasticized polymer application as bio-material in solid-state hydrogen ionic cell. *International Journal of Hydrogen Energy*, *46*(11), 8030-8039.

Kaewprachu, P., Jaisan, C., Rawdkuen, S., Tongdeesoontorn, W., & Klunklin, W. (2022). Carboxymethyl cellulose from Young Palmyra palm fruit husk: Synthesis, characterization, and film properties. *Food Hydrocolloids*, *124*, 107277.

Kim, J. S., & Lim, J. K. (2021). Mechanical properties and interfacial compatibility of functionalized carbon nanotubes as fillers for chitosan solid polymer electrolytes. *Reactive and Functional Polymers*, *166*, 105013.

Kononova, E. G., Rodnikova, M. N., Solonina, I. A., & Sirotkin, D. A. (2018). IR Spectroscopy of Ethylene Glycol Solutions of Dimethylsulfoxide. *Russian Journal of Physical Chemistry A*, *92*(7), 1308-1311.

Li, J. F. & Yang, J. S. (2019). Synthesis of Folate Mediated Carboxymethyl cellulose fatty acid ester and application drug controlled release. *Carbohydrate Polymers*, 220 (126-131).

Maitz, M. F. (2015). Applications of synthetic polymers in clinical medicine. *Biosurface and Biotribology*, *1*(3) 161-176.

Meng, N., Zhu, X., & Lian, F. (2022). Particles in composite polymer electrolyte for solid-state lithium batteries: A review. *Particuology*, *60*, 14-36.

Milani, P., França, D., Balieiro, A. G., & Faez, R. (2017). Polymers and its applications in agriculture. *Polímeros*, *27*(3), 256-266.

Mohiuddin, M., Kumar, B., & Haque, S. (2017). Biopolymer composites in Photovoltaics and Photodetectors. *Biopolymer Composites in Electronics*, 459-486.

Muchakayala, R., Song, S., Gao, S., Wang, X., Fan, Y. (2017). Structure and ion transport in an ethylene carbonate-modified biodegradable gel polymer electrolyte, *Polymer Testing*, 58, 116-125.

Perumal, P., Selvin, P. C., Selvasekarapandian, S., & Sivaraj, P. (2019) Structural and electrical properties of bio-polymer pectin with $LiClO_4$ solid electrolytes for lithium ion polymer batteries. *Materialstoday: Proceedings*, *8*(1), 196-202.

Rani, M. S. A., Rudhziah, S., Ahmad, A., & Mohamed, N. S. (2014). Biopolymer electrolyte based on derivatives of cellulose from kenaf bast fiber. *Polymers*, *6*(9), 2371-2385.

Salama, H. E., Abdel Aziz, M. S., Alsehli, M. (2019). Carboxymethyl cellulose/ sodium alginate/chitosan biguanidine hydrochloride ternary system for edible coatings. *International Journal of Biological Macromolecules*, *139*, 614-620.

Sangeetha, M., Mallikarjun, A., Aparna, Y., Reddy, M. V., Kumar, J. S., Sreekanth, T., & Reddy, M. J. (2021). Dielectric studies and AC conductivity of PVDF-HFP: LiBF4: EC plasticized polymer electrolytes. *Materials Today: Proceedings*, *44*, 2168-2172.

Selvanathan, V., Ruslan, M. H., Alkahtani, A. A. N., Amin, N., Sopian, K., Muhammad, G., & Akhtaruzzaman, M. (2021). Organosoluble, esterified starch as quasi-solid biopolymer electrolyte in dye-sensitized solar cell. *Journal of Materials Research and Technology*, *12*, 1638-1648.

Shrivastava, A. (2018). Introduction to plastics engineering. *Introduction to Plastics Engineering*, 1-16.

Sohaimy, M. I. H., Fauzi, M. J. A., & Isa, M. I. N. (2020). Electrical Behavior of Ethylene Carbonate-Plasticized Cellulose Biopolymer Electrolyte Films. *Malaysian Journal of Chemistry*, *22*(2), 22-28.

Tuan Naiwi, T. S. R., Aung, M. M., Ahmad, A., Rayung, M., Su'ait, M. S., Yusof, N. A., Wynn Lae, K. Z. (2018). Enhancement of plasticizing effect on bio-based Polyurethane Acrylate Solid Polymer Electrolyte and its properties. *Polymers*, *10*(10), 1142.

Virya, A., & Lian, K. (2021). A review of neutral pH polymer electrolytes for electrochemical capacitors: Transitioning from liquid to solid devices. *Materials Reports: Energy*, *1*(1) 100005.

Yazdani, N., Garcia, E. C., & Riad, M. (2018). Field assessment of concrete structures rehabilitated with FRP. *Eco-Efficient Repair and Rehabilitation of Concrete Infrastructures*, 171-194.

Zainuddin, N., Rasali, N., Mazuki, N., Saadiah, M., & Samsudin, A. (2020). Investigation on favourable ionic conduction based on CMC-K carrageenan proton conducting hybrid solid bio-polymer electrolytes for applications in EDLC. *International Journal of Hydrogen Energy*, *45*(15), 8727-8741.